

Research Article

Development of an Omnidirectional-Capable Electromagnetic Shock Wave Generator for Lipolysis

Ming Hau Chang and San Yih Lin

Department of Aeronautics and Astronautics, National Cheng Kung University, No. 1, University Road, Tainan City 701, Taiwan

Correspondence should be addressed to Ming Hau Chang; changminghau@gmail.com

Received 23 January 2017; Revised 18 March 2017; Accepted 9 April 2017; Published 24 May 2017

Academic Editor: Saverio Affatato

Copyright © 2017 Ming Hau Chang and San Yih Lin. This is an open access article distributed under the Creative Commons Attribution License, which permits unrestricted use, distribution, and reproduction in any medium, provided the original work is properly cited.

Traditional methods for adipose tissue removal have progressed from invasive methods such as liposuction to more modern methods of noninvasive lipolysis. This research entails the development and evaluation of an omnidirectional-capable flat-coil electromagnetic shock wave generator (EMSWG) for lipolysis. The developed EMSWG has the advantage of omnidirectional-capable operation. This capability increases the eventual clinical usability by adding three designed supports to the aluminum disk of the EMSWG to allow omnidirectional operation. The focal pressures of the developed EMSWG for different operating voltages were measured, and its corresponding energy intensities were calculated. The developed EMSWG was mounted in a downward orientation for lipolysis and evaluated as proof of concept. In vitro tests on porcine fatty tissues have been carried out. It is found that at a 6 kV operating voltage with 1500 shock wave exposures, a 2 cm thick subcutaneous hypodermis of porcine fatty tissue can be ruptured, resulting in a damaged area of 1.39 mm². At a 6.5 kV operating voltage with 2000 shock wave exposures, the damaged area is increased to about 5.20 mm², which can be enlarged by changing the focal point location, resulting in significant lipolysis for use in clinical applications.

1. Introduction

Human obesity is problematic from the viewpoints of both health and aesthetics. Previously, removing excessive fatty tissue involved invasive liposuction methods which posed a risk of excessive bleeding. Side effects such as cellulite might be induced [1–3]. On the other hand, noninvasive methods of lipolysis can lower the risks and are preferred [4–6]. Common noninvasive appliances currently used for body contouring are ultrasonic devices, such as Liposonix® (Solta Medical Inc., USA), UltraShape® (Syneron and Candela Inc., USA) and Cellactor® (Storz Medical Inc., CH) [7–10]. A continuous repetition of high intensity-focused ultrasound might induce lesions or overheating which leads to cavity generation and tissue dehydration [11]. Similarly, low-level laser therapy (LLLT) is a new modality for body contouring. However, some common side effects of LLLT include pain, scarring, and skin pigmentation [12].

The medical application of extracorporeal shock waves for ailments such as renal stones, gallbladder stones, and musculoskeletal disorders has been quite successful [13–17] for the past 20 years or more. Studies on medical applications of shock waves in diverse areas are progressing, such as the treatment of myocardial ischemia [18, 19], diabetes, atherosclerosis, and venous insufficiency as well as in revascularization [20] and soft wound healing [21] and in research on the proliferation of mesenchymal stem cells [22]. When shock waves are applied for lipolysis, temperature increase in the fatty tissue treated with focused shock waves is almost negligible [23–25]. There are three types of extracorporeal shock wave lithotripters: electrohydraulic, electromagnetic, and piezoelectric [21, 23, 24]. The mechanism of lysing adipocytes with extracorporeal shock waves is via cavitation produced by shock waves [6, 23, 24]. Cavitation is the process of gaseous bubble formation in liquid. As negative pressure occurs in water, it induces a cavitation phenomenon which

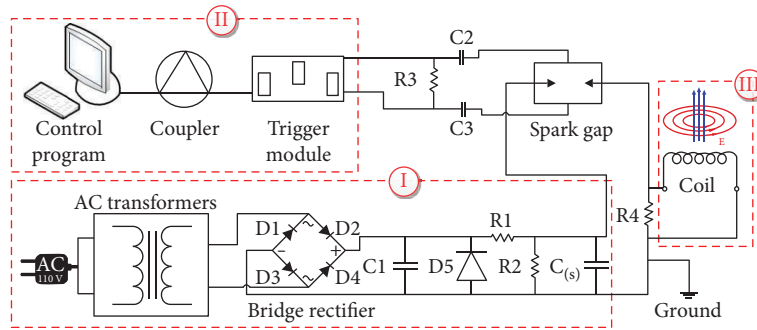


FIGURE 1: Experimental setup schematic for EMSWG.

results in expanding bubbles and toroidal collapse near the target surface. These bubbles are formed around the focal region of the focused shock wave. When the bubbles collapse, they emit high-speed water microjets which impact nearby adipocyte membranes [26, 27].

Liang et al. previously had used extracorporeal shock waves to rupture porcine fatty tissues [28, 29]. Their in vitro test results showed that lipolysis by shock waves was feasible. In Liang's works, the electromagnetic shock wave generator (EMSWG) was arranged in a vertical direction so that shock waves were generated and propagated only in an upward direction. For clinical purposes, a unidirectional operation shock wave generator is inconvenient for medical treatment. In their EMSWG, a shock wave is generated by an accelerated moving metal disk in water. The moving disk is returned to the original position by gravity. This limitation is remedied in this work.

In this study, an electromagnetic-type shock wave generator is constructed for lipolysis using a similar mechanism to existing extracorporeal shock wave generator design [6, 13], but having an advantage of possible omnidirectional operation. The efficacy of the refined device is evaluated by measuring the focal pressure of the focused shock wave and by calculating the corresponding energy intensity. Finally, the histological effects on the treated porcine fat tissues are examined.

2. Experimental Methods

2.1. Experimental Setup. The setup of an experimental lipotripter is briefly described below. There are three major parts of the experimental system: (I) a power charging system, (II) a signal control system, and (III) a shock wave generator. The system is depicted in Figure 1.

The power charging system converts alternating current (AC) voltage into direct current (DC) voltage in the range of 0–6.5 kV using an autotransformer and a bridge rectifier. The DC power is stored in several high-voltage capacitors connected to a triggered spark gap (PerkinElmer Inc., USA). The triggered spark gap can be operated in the voltage range of 5–15 kV, which is suitable for capacitor-switching applications such as medical lithotripters.

The signal control system consists of a computer, an analog output module (NI 9263, National Instruments, USA), and a trigger module (PerkinElmer Inc., USA). The signal

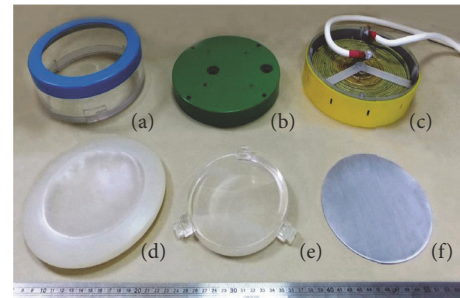


FIGURE 2: Components of EMSWG: (a) acrylic container, (b) coil cover, (c) coil and coil housing, (d) soft cover, (e) acoustic lens, and (f) aluminum disk.

control program is written using the LabVIEW package (National Instruments, USA). The control program has several settable parameters, such as operating voltage, frequency, and total number of shock wave exposures. The trigger module allows the triggering of the spark gap connected to the shock wave generator.

The electromagnetic shock wave generator in this study consists of a flat coil electromagnet, an aluminum disk, an acoustic lens, and a soft cover. The soft cover comes into contact with the patient. The aluminum disk is accelerated to generate shock waves in liquid when the flat coil is charged. For durability, the acoustic lens is designed to be flat on one side and parabolic on the other to avoid brittleness stemming from the thinness of the lens. The effective focus is found experimentally by locating the peak pressure point of a focused shock wave. The acoustic lens in this study has an effective focal length equal to its geometric focal length of 9 cm [29].

A 30 × 30 × 30 cm rectangular tank was constructed and filled with reverse osmosis (RO) water to accommodate the aforementioned shock wave generator for pressure measurements. RO water is used because it has few impurities to interfere with shock wave transmission. A polyvinylidene difluoride (PVDF) needle-type pressure sensor (SN 1841, Precision Acoustics Inc., UK) was connected through a DC coupler to measure the peak pressure at the focal point. The DC coupler interfaced with an oscilloscope (Agilent Technologies Co., USA) to display the voltage waveform. The measured voltage wave data allowed the calculation of peak

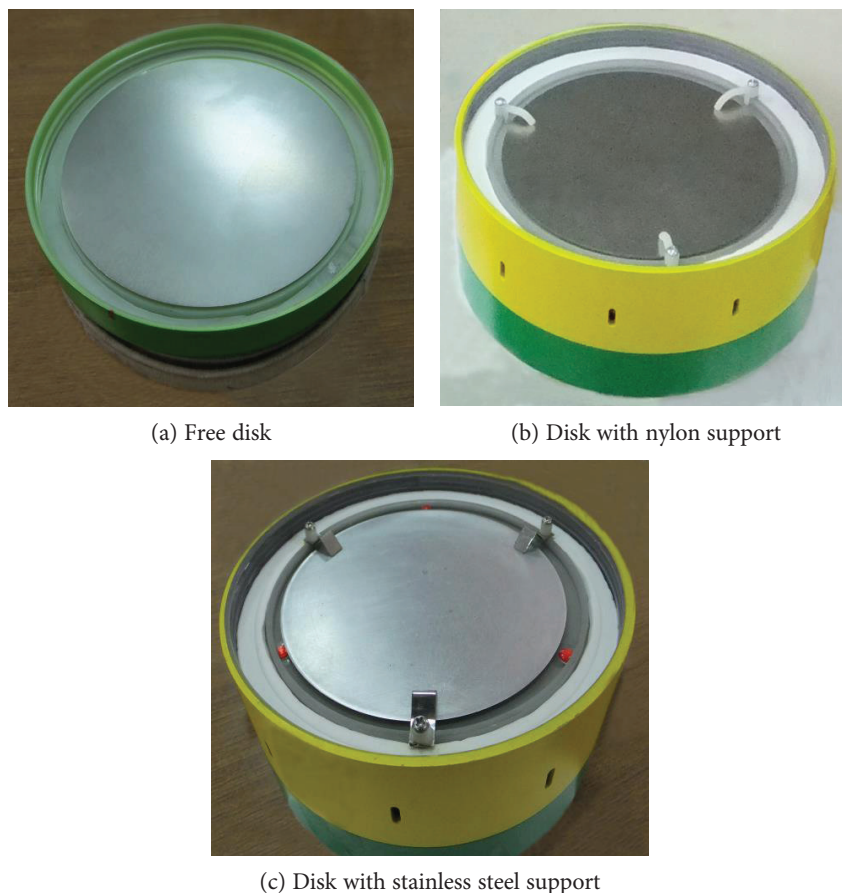


FIGURE 3: Aluminum disks without and with supports: (a) free disk only having upward arrangement, (b) nylon, and (c) steel supports used for aluminum disk.

pressure and associated energy intensity. The rectangular water tank was reutilized for the lipolysis experiments on the porcine fatty tissues. After hematoxylin and eosin staining, treated tissues were histologically examined to see the effects of the shock waves.

2.2. The Electromagnetic Shock Wave Generator

2.2.1. Components of the EMSWG. The functional elements of the EMSWG consist of a circular acrylic container (Figure 2(a)), a flat-shaped electromagnetic coil inside the coil housing (Figure 2(c)), a soft cover (Figure 2(d)), an acoustic lens (Figure 2(e)) and a 1 mm 6061-0 aluminum disk (Figure 2(f)). A coil cover (Figure 2(b)) protects the 22-turn electromagnetic coil. The aluminum disk abuts the coil housing. The acoustic lens with a radius of 6.1 cm is fixed at a distance of approximately 9 mm from the aluminum disk. The circular acrylic container filled with RO water serves as the shock wave medium housing. One end of the container can be screwed onto the coil housing. The other end is connected to the flexible soft cover which physically contacts the target tissue.

2.2.2. Omnidirectional EMSWG. For clinical use, omnidirectional operation of an EMSWG would be much more convenient. To this end, the EMSWG is designed to maintain

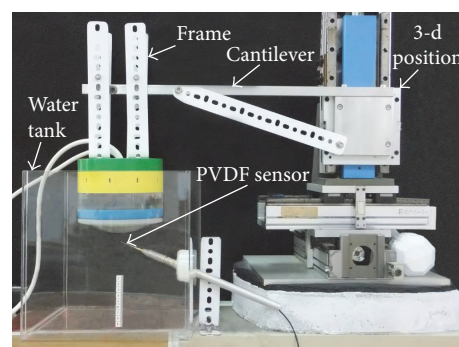


FIGURE 4: Experimental setup for pressure measurements.

viability of the shock wave generation in various orientations. Though in this work, only the downward orientation is tested to determine initial feasibility of the proposed design. The design uses three small equidistant supports (Figures 3(b) and 3(c)) to constrain the free aluminum disk (Figure 3(a)). Two support materials were tested. The first design incorporated small curved nylon rods as supports, as shown in Figure 3(b). Unfortunately, the nylon rods would deform after about 500 shock waves due to material fatigue. Thus, three 301 stainless steel supports were used in the revised design, as shown in

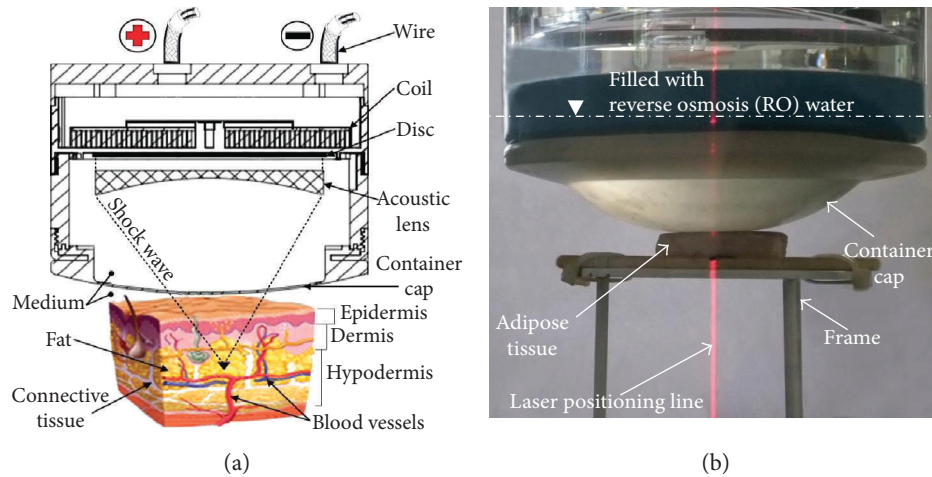


FIGURE 5: (a) Schematic diagram of an omnidirectional EMSWG and (b) setup used for in vitro experiments.

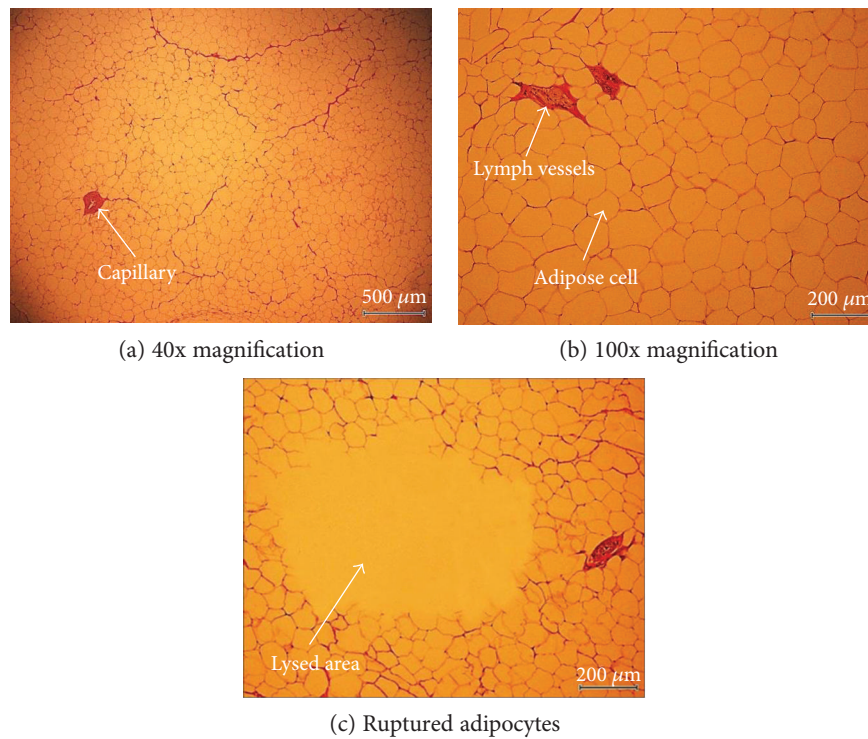


FIGURE 6: Histological examination after H&E staining of normal porcine adipocyte specimen at (a) 40x magnification. Examination of (b) normal and (c) shock wave-treated specimens at 100x magnification.

Figure 3(c). These steel supports did not deform after repeated use.

2.3. Pressure Measurements

2.3.1. Measurement of Peak Pressures. For measuring the peak pressures of focused shock waves, the omnidirectional-capable EMSWG was suspended by a cantilevered three-dimensional positioning platform in a water tank, as shown in Figure 4. The needle tip of a 0.5 mm PVDF hydrophone was placed at the effective focal point of the acoustic lens. The probe sensitivity is about 300 nV/Pa, and the sensitivity

tolerance variation is approximately ± 3 dB. The operating voltage of the omnidirectional-capable EMSWG was set in the range of 5–6.5 kV with increments of 0.5 kV. Twenty pressure measurement samples were taken for defining the focal pressure at the shock wave exposure frequency of 1 Hz for each tested operating voltage. After obtaining the peak pressure, energy intensity was calculated.

2.3.2. Calculation of Energy Intensity. Energy intensity is defined as the integral of pressure squared and divided by sound impedance.

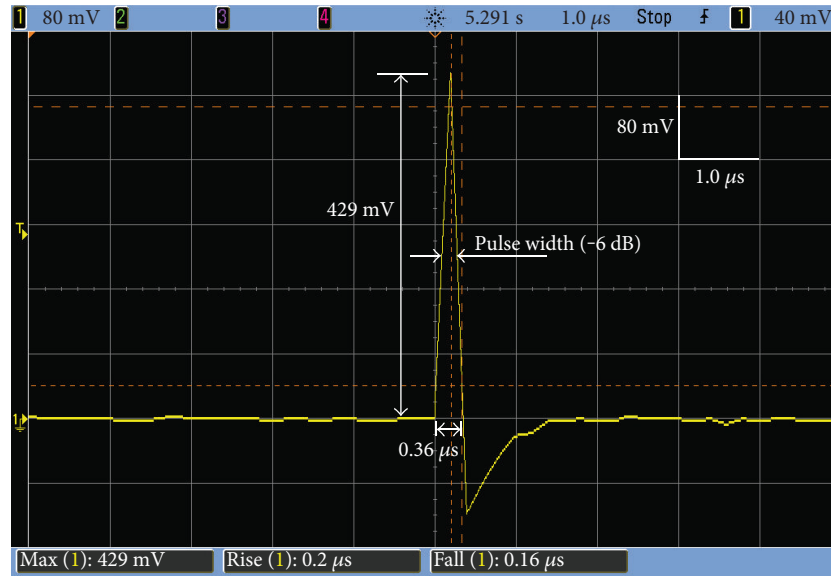


FIGURE 7: Focal pressure characteristics of a single pressure pulse measured by a PVDF hydrophone.

$$I = \left[\frac{1}{\rho c} \right] \cdot \int p^2 dt, \quad (1)$$

where I is the energy intensity, ρ the water density, p the pressure, t the time, and c the sound speed in water.

2.4. In Vitro Tests on Porcine Fatty Tissues. Since the structure of porcine fatty tissue is similar to that of humans, tissues of the domestic pig (*Sus scrofa domestica*) were used in this study. Normal human skin consists of the epidermis, dermis, and hypodermis, as seen in Figure 5(a). The epidermis and dermis combined have a thickness of 2–4 mm. Human fat cells are mainly stored in the hypodermis, at about 1–2 cm in depth. This corresponds to the treatment range of clinical devices such as the UltraShape® (about 1.5 cm below the skin) and Liposonix (about 1.3 cm below the skin). Figure 5 shows a cross section diagram of the developed omnidirectional-capable EMSWG. The developed EMSWG is oriented so that the target adipose tissue is beneath the soft cover. The EMSWG and target tissue were submerged into the water tank. A red 650 nm laser positioning device (>5 mW) was used to mark the focal point location in the treated tissue, as shown in Figure 5(b).

2.5. Histological Examination. In order to examine the damage extent of the treated porcine fatty tissues, the 2 cm treated tissues were fixed and dehydrated by being packed in a cassette and submerged in a formalin solution for three days. After the processes of clearing and infiltration, the treated tissues were embedded and sliced into 3 μm thick slices. The final process of hematoxylin and eosin was carried out for histological examination through a microscope. Figure 6 shows the comparison of the normal and ruptured porcine adipocytes. Figure 6(a) shows a $\sim 3.5 \times 2.5 \text{ mm}^2$ picture of normal porcine adipocytes at 40x magnification. Figure 6(b) shows a $\sim 1.4 \times 0.99 \text{ mm}^2$ picture of normal porcine adipocytes at 100x magnification. In Figure 6(b), the regular arrangement

of the normal adipocytes is clearly seen. In Figure 6(c), the empty region indicates ruptured adipocytes.

3. Results and Discussion

3.1. Pressure Measurements. The developed EMSWG is arranged in a downward position. The measured focal pressure profile of a typical focused shock wave is shown in Figure 7. The 429 mV peak of the pressure pulse corresponds to the peak pressure of 1.41 MPa and the energy intensity of 0.081 mJ/mm^2 at the operating voltage of 6.5 kV. The duration time of the focal pressure profile is 0.36 μs . The rise time is 0.2 μs and 0.16 μs for the fall time.

3.2. Experimental Results of In Vitro Tests

3.2.1. Effect of Adipose Tissue Thickness. For studying the effect of adipose tissue thickness, the operating voltages were set to 5.5–6.5 kV with increments of 0.5 kV. The RO water medium has an acoustic impedance of approximately 1.4 M rayls, which is close to that of the blood (at approximately 1.6 M rayls). Shock wave experiments without targets served as the control cases. The measured peak pressures for the controls are used for comparison with the adipose tissue experiments. In order to calculate the extent of energy intensity loss through the treated fatty tissue, skinless adipose tissue specimens of three different thicknesses (1, 2, and 3 cm) were selected so that the effective focal point was located at 1–2 cm below the surface of the treated tissue.

The measured peak pressure and energy intensity with error bars at the focus for different tested samples and operating voltages are shown in Figure 8. Note that the PVDF needle hydrophone tip was positioned right below the adipose tissue. Table 1 shows the measured peak pressures for various treated porcine adipose tissues. Twenty pressure data points were used. The average peak pressure at 5.5 kV for the water case is 0.99 MPa, 0.93 MPa for 1 cm thick adipose

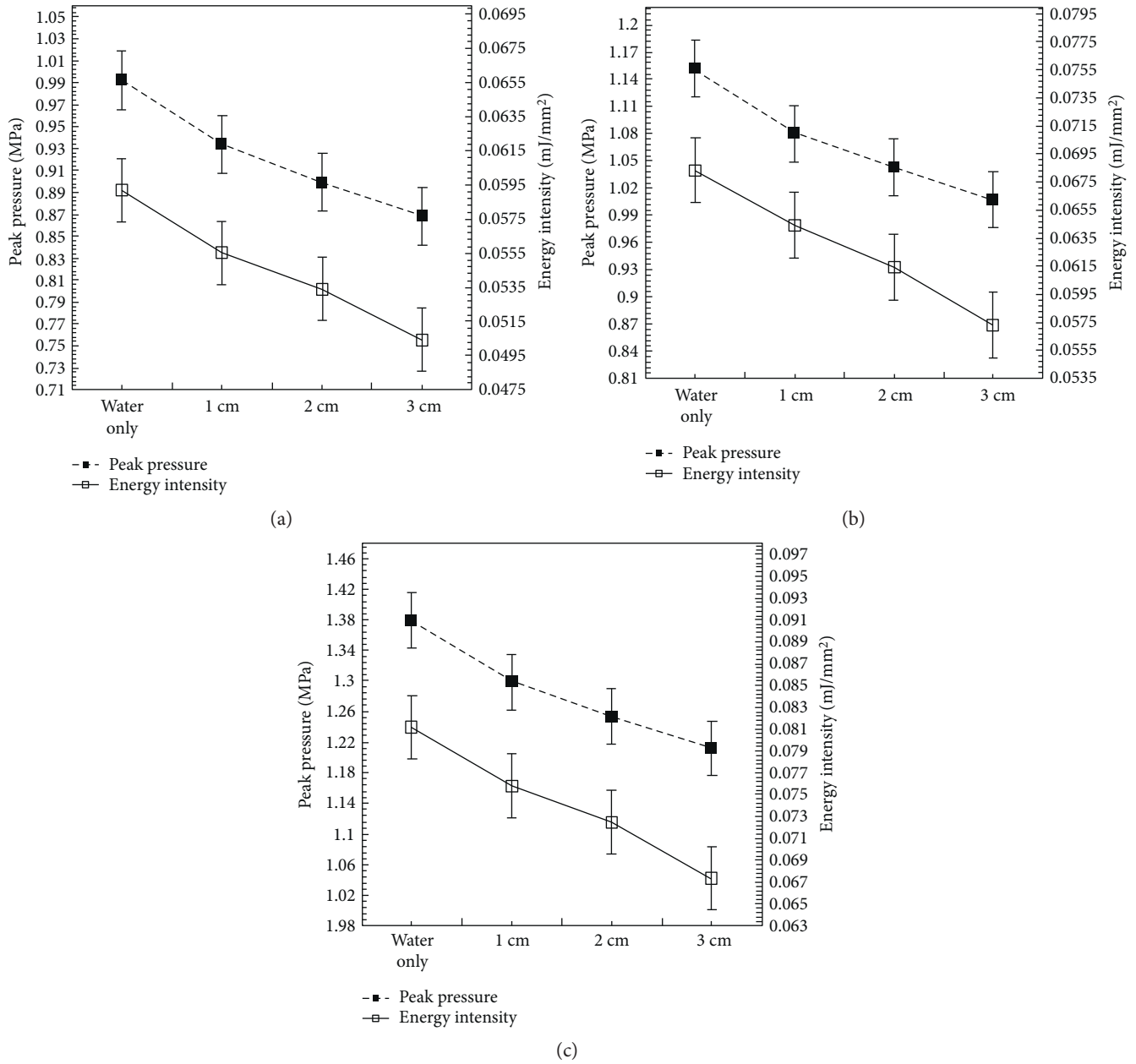


FIGURE 8: The peak pressure and energy intensity with error bar at the focus for different tested samples of porcine adipose tissues without the skin at operating voltages of (a) 5.5 kV, (b) 6 kV, and (c) 6.5 kV.

tissue, 0.9 MPa for 2 cm thickness, and 0.87 MPa for 3 cm thickness. The recorded peak pressure loss of the 1 cm thick adipose tissue at 5.5 kV is 6.1% less compared to the control, with a 6.1% reduction at 6 kV and 6.5% reduction at 6.5 kV. For 2 cm thick adipose tissue, the measured peak pressure is 0.9 MPa at 5.5 kV, which is a 9.1% reduction compared to the peak pressure of the control case. Operating voltage of 6 kV results in a 9.6% reduction and 6.5 kV results in a 9.4% reduction.

For adipose tissue of 3 cm thickness, the measured peak pressure is 0.87 MPa at 5.5 kV which is a 12.1% reduction compared to the peak pressure of the control case, with a 12.2% reduction at 6 kV, and a 12.3% reduction at 6.5 kV. The corresponding energy intensities for

various cases are shown in Table 2. The trends of the peak pressure and energy intensity losses due to adipose tissue thickness are shown in Figure 8.

In the same way, one can study the effect of energy intensity through adipose tissue thickness. It is found that the reduction in the energy intensity for the 1 cm thickness is 5.1% at 5.5 kV, 5.9% at 6 kV, and 6.2% at 6.5 kV. For the 2 cm thickness, the reduction in the energy intensity is 10.2% at 5.5 kV, 10.3% at 6 kV, and 11.1% at 6.5 kV. For the 3 cm thickness, the reduction in the energy intensity is 15.3% at 5.5 kV, 16.2% at 6 kV and 17.3% at 6.5 kV.

For the effects of shock wave exposures over the range of 5.5–6.5 kV, the peak pressure and energy intensity have a proportional relationship regardless of the operating voltage.

TABLE 1: Average peak pressures of focused shock waves for various specimens.

Specimen	RO water				1 cm thick adipose tissue			2 cm thick adipose tissue			3 cm thick adipose tissue		
Operating voltage (kV)	5	5.5	6	6.5	5.5	6	6.5	5.5	6	6.5	5.5	6	6.5
Average (MPa) \pm SD	0.87 \pm 0.004	0.99 \pm 0.003	1.15 \pm 0.067	1.38 \pm 0.06	0.93 \pm 2.37	1.08 \pm 2.57	1.29 \pm 1.74	0.9 \pm 1.1	1.04 \pm 2.77	1.25 \pm 0.91	0.87 \pm 1.07	1.01 \pm 1.19	1.21 \pm 1.07
Energy intensity change (%)	n/a				-6.1	-6.1	-6.5	-9.1	-9.6	-9.4	-12.1	-12.3	-12.3

TABLE 2: Average energy intensities of focused shock waves for various specimens.

Specimen	RO water				1 cm thick adipose tissue			2 cm thick adipose tissue			3 cm thick adipose tissue		
Operating voltage (kV)	5	5.5	6	6.5	5.5	6	6.5	5.5	6	6.5	5.5	6	6.5
Average (mJ/mm ²) \pm SD	0.052 \pm 0.6e-3	0.059 \pm 0.4e-3	0.068 \pm 0.5e-3	0.081 \pm 0.5e-3	0.056 \pm 0.28e-3	0.064 \pm 0.27e-3	0.076 \pm 0.18e-3	0.053 \pm 0.19e-3	0.061 \pm 0.15e-3	0.072 \pm 0.21e-3	0.05 \pm 0.29e-3	0.057 \pm 0.20e-3	0.067 \pm 0.24e-3
Energy intensity change (%)	n/a				-5.1	-5.9	-6.2	-10.2	-10.3	-11.1	-15.3	-16.2	-17.3

Both the peak pressure and energy intensity are inversely related versus the specimen thickness. Thus, the effect is proportionally decreased with the increase of tissue thickness. Moreover, it was also found that when using fatty tissues of 3 cm thickness, the energy intensity was reduced by about 10–18%, therefore reducing the performance of lipolysis treatment. In general, human adipose tissues are mainly stored in the hypodermis, so the effective focal point is generally 1–2 cm below the skin of a patient undergoing a clinical application. Therefore, porcine fatty tissues of 2 cm thickness were selected for further study.

3.2.2. Evaluation of the Affected Area. Among noninvasive clinical treatments currently used for lipolysis or body contouring, the main treatment depth for adipose tissue is approximately 2 cm due to the fact that the subcutaneous hypodermis region of the abdomen is located approximately 2 cm deep. For this reason, the specimen size of porcine fatty tissue was set at 2 cm thick. The amount of affected adipose tissue is basically dependent on two parameters: the operating voltage and the number of shock wave exposures.

The adipose tissues treated with shock waves were processed through paraffin block sectioning as well as hematoxylin and eosin staining. The extent of adipose tissue lysis was observed through a microscope. As seen from Figure 6(c), there is a region of ruptured adipose tissue after shock wave treatment. In order to easily identify the region affected by shock waves, the region of ruptured adipose tissue is shaded in subsequent images.

In order to estimate the extent of the damaged area, specimens of the treated adipose tissue were examined after H&E staining. Figure 9 shows images of the ruptured adipose tissue at 40x magnification for different shock wave exposures at 6 kV. The examined adipose tissue specimens were about $3.5 \times 2.5 \text{ mm}^2$ through a microscope. It is found that the lysed

(shaded) area is about 0.24 mm^2 , with approximately 28 ruptured adipocytes for 500 shock waves (Figure 9(a)). For 1000 shock waves, the damaged area is at least 0.46 mm^2 , because some damage is out of the image range, with approximately 54 ruptured adipocytes (Figure 9(b)). For 1500 shock waves, the lysed area is at least 1.39 mm^2 , with approximately 164 ruptured adipocytes (Figure 9(c)). For 2000 shock waves, the lysed area totaled at least 2.35 mm^2 , with approximately 270 ruptured adipocytes (Figure 9(d)), as shown in Table 3.

Figures 9(e), 9(f), 9(g), and 9(h) show 40x magnification pictures of the lysed adipose tissues at the 2 cm depth after H&E staining for different shock wave exposures at 6.5 kV. For 500 shock waves, the lysed area is at least 2.73 mm^2 , with approximately 320 ruptured adipocytes (Figure 9(e)). For 1000 shock waves, the lysed area is at least 3.80 mm^2 , with approximately 448 ruptured adipocytes (Figure 9(f)). For 1500 shock waves, the lysed area is at least 4.36 mm^2 , with approximately 512 ruptured adipocytes (Figure 9(g)). Finally, for 2000 shock waves, there is at least 5.20 mm^2 lysed area, with approximately 610 ruptured adipocytes, as shown in Figure 9(h). Table 3 summarizes the data pertaining to Figure 9.

4. Conclusion

In consideration of the clinical use of an electromagnetic shock wave generator for lipolysis, an omnidirectional EMSWG proof of concept has been developed and evaluated. The developed EMSWG can be operated not only in an upward position but also in a downward position. Hence, the functionality of the EMSWG is enhanced.

The performance of the omnidirectional-capable EMSWG has been histologically examined through in vitro testing of the lipolysis effect on porcine adipose tissues located at a depth of 2 cm. The affected region of the treated

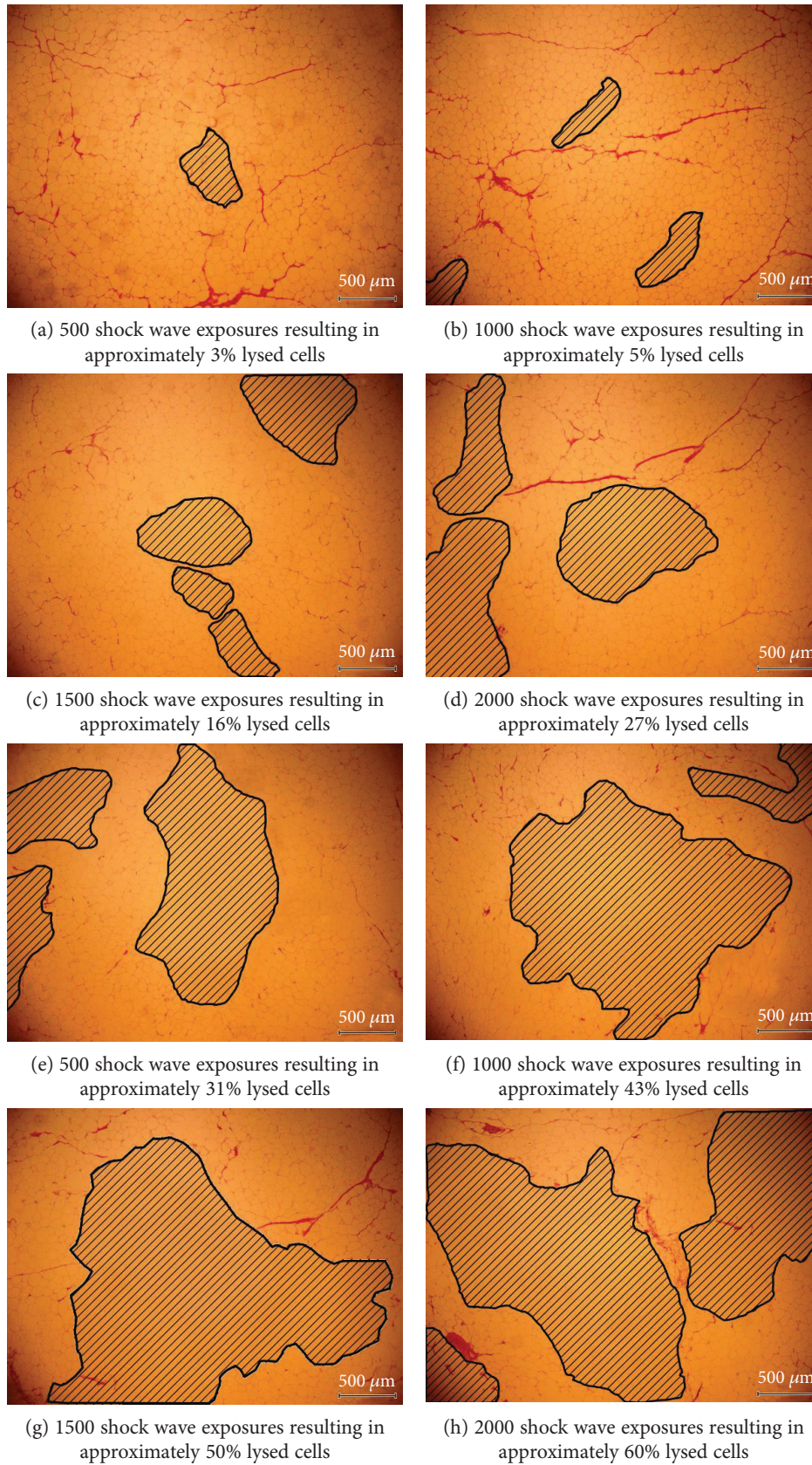


FIGURE 9: Adipose tissue specimens measuring $3.5 \times 2.5 \text{ mm}^2$ with ruptured adipocytes (shaded areas) after H&E staining for various number of shock wave exposures at 6 kV (a–d) and 6.5 kV (e–h). These are representative samples at 2 cm depth with 40x magnification.

TABLE 3: Effect of lipolysis at 6 kV and 6.5 kV with various number of shock wave exposures on $3.5 \times 2.5 \text{ mm}^2$ sized specimens.

Operating voltage (kV)	6				6.5			
Number of shock wave exposures	500	1000	1500	2000	500	1000	1500	2000
Lysed area (mm^2)	0.24	0.46	1.39	2.35	2.73	3.80	4.36	5.20
Lysed area (%)	2.7	5.3	15.9	26.9	31.2	43.4	49.8	59.4
Ruptured adipocytes	28	54	164	277	321	448	512	611

adipose tissue is dependent on the operating voltage and the number of shock wave exposures. Effective lipolysis results at operating voltages of at least 6 kV. If the operating voltage is less than 6 kV, adipose tissue damage is almost negligible. At operating voltages of 6 kV or greater, some extent of damage on the treated adipose tissues is observable. In general, the use of operating voltages higher than 6.5 kV may cause side effects on the patient skin. However, additional shock wave exposure at a lower operating voltage can achieve the same treatment outcome. For 2 cm thick fatty tissues at 6 kV operating voltage, 500, 1000, 1500, and 2000 shock wave exposures yield lysed areas of percentages of about 2.7%, 5.3%, 15.9%, and 26.9%, respectively. As expected, increasing the operating voltage enhances lipolysis effects. At 6.5 kV, 500, 1000, 1500, and 2000 shock wave exposures yield larger lysed area of percentages of about 31.2%, 43.4%, 49.8%, and 59.4%, respectively.

These initial results are promising, and this approach warrants further study for possible clinical application as a noninvasive omnidirectional electromagnetic-type shock wave generator for lipolysis.

Conflicts of Interest

The authors declare that there is no conflict of interests regarding the publication of this paper.

Acknowledgments

The support of the Ministry of Science and Technology, R. O. C., MOST 103-2221-E-269-001 and MOST 103-2221-E-006-193-MY3, is gratefully acknowledged. The authors are indebted to Professor S. M. Liang for the advice and detailed discussion on this manuscript.

References

- [1] R. J. Rohrich, S. J. Beran, J. M. Kenkel, W. P. Adams, and F. DiSpaltro, "Extending the role of liposuction in body contouring with ultrasound-assisted liposuction," *Plastic and Reconstructive Surgery*, vol. 101, no. 4, pp. 1090–1102, 1998.
- [2] A. F. Del Campo, E. R. Allegretti, J. A. Fernandes Filho, and C. B. Gordon, "Liposuction: procedure for focal volume reduction and body contour remodeling," *World Journal of Surgery*, vol. 22, no. 9, pp. 981–986, 1998.
- [3] K. Sumiyama, K. Utsunomiya, T. Ohya et al., "A pilot study on ultrasound-assisted liposuction of the greater omentum in porcine models," *Minimally Invasive Therapy & Allied Technologies*, vol. 21, no. 2, pp. 71–77, 2012.
- [4] N. Sadick and C. Magro, "A study evaluating the safety and efficacy of the velasMOOTH (TM) system in the treatment of cellulite," *Journal of Cosmetic and Laser Therapy*, vol. 9, no. 1, pp. 15–20, 2007.
- [5] F. Angehrn, C. Kuhn, and A. Voss, "Can cellulite be treated with low-energy extracorporeal shock wave therapy?" *Clinical Interventions in Aging*, vol. 2, no. 4, pp. 623–630, 2007.
- [6] C. Kuhn, F. Angehrn, O. Sonnabend, and A. Voss, "Impact of extracorporeal shock waves on the human skin with cellulite: a case study of an unique instance," *Clinical Interventions in Aging*, vol. 3, no. 1, pp. 201–210, 2008.
- [7] J. Moreno-Moraga, T. Valero-Altés, A. M. Riquelme, M. I. Isarria-Marcosy, and J. R. De La Torre, "Body contouring by non-invasive transdermal focused ultrasound," *Lasers in Surgery and Medicine*, vol. 39, no. 4, pp. 315–323, 2007.
- [8] K. M. Coleman, W. P. Coleman, and A. Benchetrit, "Non-invasive, external ultrasonic lipolysis," *Seminars in Cutaneous Medicine and Surgery*, vol. 28, no. 4, pp. 263–267, 2009.
- [9] S. A. Brown, L. Greenbaum, S. Shtukmaster, Y. Zadok, S. Ben-Ezra, and L. Kushkuley, "Characterization of nonthermal focused ultrasound for noninvasive selective fat cell disruption (lysis): technical and preclinical assessment," *Plastic and Reconstructive Surgery*, vol. 124, no. 1, p. 10, 2009.
- [10] M. A. Adatto, R. Adatto-Neilson, P. Novak, A. Krotz, and G. Haller, "Body shaping with acoustic wave therapy AWT®/EPAT®: randomized, controlled study on 14 subjects," *Journal of Cosmetic & Laser Therapy*, vol. 13, no. 6, pp. 291–296, 2011.
- [11] A. Shalom, I. Wiser, S. Brawer, and H. Azhari, "Safety and tolerability of a focused ultrasound device for treatment of adipose tissue in subjects undergoing abdominoplasty: a placebo-control pilot study," *Dermatologic Surgery*, vol. 39, no. 5, pp. 744–751, 2013.
- [12] M. S. Nestor, J. Newburger, and M. B. Zarraga, "Body contouring using 635-nm low level laser therapy," *Seminars in Cutaneous Medicine and Surgery*, vol. 32, no. 1, pp. 35–40, 2013.
- [13] M. Delius, "Medical applications and bioeffects of extracorporeal shock waves," *Shock Waves*, vol. 4, no. 2, pp. 55–72, 1994.
- [14] R. Leistner, G. Wendt-Nordahl, R. Grobholz et al., "A new electromagnetic shock-wave generator "SLX-F2" with user-selectable dual focus size: ex vivo evaluation of renal injury," *Urological Research*, vol. 35, no. 4, pp. 165–171, 2007.
- [15] C. J. Wang, "Extracorporeal shockwave therapy in musculoskeletal disorders," *Journal of Orthopaedic Surgery and Research*, vol. 7, no. 1, p. 11, 2012.
- [16] M. Senyucel, O. Boybeyi, S. Ayva et al., "Evaluation of contralateral kidney, liver and lung after extracorporeal shock wave lithotripsy in rabbits," *Urolithiasis*, vol. 41, no. 5, pp. 431–436, 2013.
- [17] P. Romeo, V. Lavanga, D. Pagani, and V. Sansone, "Extracorporeal shock wave Therapy in musculoskeletal disorders: a review," *Medical Principles and Practice*, vol. 23, no. 1, pp. 7–13, 2014.

- [18] J. G. Mancini, A. Neisius, N. Smith et al., "Assessment of a modified acoustic lens for electromagnetic shock wave lithotripters in a swine model," *The Journal of Urology*, vol. 190, no. 3, pp. 1096–1101, 2013.
- [19] Y. Fukumoto, A. Ito, T. Uwatoku et al., "Extracorporeal cardiac shock wave therapy ameliorates myocardial ischemia in patients with severe coronary artery disease," *Coronary Artery Disease*, vol. 17, no. 1, pp. 63–70, 2006.
- [20] R. Mittermayr, J. Hartinger, V. Antonic et al., "Extracorporeal shock wave therapy (ESWT) minimizes ischemic tissue necrosis irrespective of application time and promotes tissue revascularization by stimulating angiogenesis," *Annals of Surgery*, vol. 253, no. 5, pp. 1024–1032, 2011.
- [21] V. Antonic, R. Mittermayr, W. Schaden, and A. Stojadinovic, "Evidence supporting extracorporeal shockwave therapy for acute and chronic soft tissue wounds," *Wounds-a Compendium of Clinical Research and Practice*, vol. 23, no. 7, pp. 204–215, 2011.
- [22] O. Raabe, K. Shell, A. Goessl et al., "Effect of extracorporeal shock wave on proliferation and differentiation of equine adipose tissue-derived mesenchymal stem cells in vitro," *American Journal of Stem Cells*, vol. 2, no. 1, pp. 62–73, 2013.
- [23] J. A. Ogden, A. Toth-kischkat, and R. Schultheiss, "Principles of shock wave therapy," *Clinical Orthopaedics and Related Research*, vol. 28, no. 387, pp. 8–17, 2001.
- [24] S. McClure and C. Dorfmueller, "Extracorporeal shock wave therapy: theory and equipment," *Clinical Techniques in Equine Practice*, vol. 2, no. 4, pp. 348–357, 2003.
- [25] R. Mittermayr, V. Antonic, J. Hartinger et al., "Extracorporeal shock wave therapy (ESWT) for wound healing: technology, mechanisms, and clinical efficacy," *Wound Repair and Regeneration*, vol. 20, no. 4, pp. 456–465, 2012.
- [26] I. Chilibon, M. Wevers, J. P. Lafaut, and L. Baert, "Cavitation role in extracorporeal shock wave lithotripsy," *Journal of Optoelectronics and Advanced Materials*, vol. 8, no. 1, pp. 235–237, 2006.
- [27] O. Supponen, P. Kobel, D. Obreschkow, and M. Farhat, "The inner world of a collapsing bubble," *Physics of Fluids*, vol. 27, no. 9, p. 091113, 2015.
- [28] S.-M. Liang, C.-N. Yeh, J.-J. Yan, L.-R. Wan, and J.-W. Lee, "An in-vitro experiment on lysing adipose tissue by shock waves," *Journal of Medical and Biological Engineering*, vol. 28, no. 4, pp. 203–209, 2008.
- [29] S. M. Liang, M. H. Chang, and Z. Y. Yang, "Development and performance evaluation of an electromagnetic-type shock wave generator for lipolysis," *Review of Scientific Instruments*, vol. 85, no. 1, p. 015113, 2014.